RESEARCH NOTE

A High-Resolution Transmission Electron Microscopy Study of the Influence of Fluorine on the Morphology and Dispersion of WS$_2$ in Sulfided W/Al$_2$O$_3$ and NiW/Al$_2$O$_3$ Catalysts

Mingyong Sun,*,[1] Patricia J. Kooyman,† and Roel Prins*,[2]

*Laboratory for Technical Chemistry, Swiss Federal Institute of Technology (ETH), 8093 Zurich, Switzerland; and †National Centre for High Resolution Electron Microscopy, Delft University of Technology, Rotterdamseweg 137, 2628 AL Delft, The Netherlands

The morphology of WS$_2$ on sulfided tungsten and nickel–tungsten catalysts supported on alumina and fluorinated alumina, prepared from ammonium metatungstate and ammonium tetrathiotungstate, was investigated by means of high-resolution transmission electron microscopy. The sulfided catalysts prepared from ammonium metatungstate contain mainly single-layered WS$_2$ slabs, while those prepared from ammonium tetrathiotungstate contain more multilayered WS$_2$ slabs. Incorporation of nickel increases the stacking and stabilizes small WS$_2$ crystallites. Fluorination of the alumina support increases the fraction of multilayered WS$_2$ slabs and increases the WS$_2$ slab diameter. © 2002 Elsevier Science (USA)

Key Words: high-resolution transmission electron microscopy; HRTEM; fluorination; W/Al$_2$O$_3$; NiW/Al$_2$O$_3$.

INTRODUCTION

The addition of fluorine to alumina enhances the activity of acid-catalyzed reactions (1–3), cracking and isomerization reactions (4, 5), and hydrodesulfurization (HDS) and hydrodenitrogenation (HDN) reactions of hydrotreating catalysts (4–6). The interpretation of the effect of fluorine on hydrotreating catalysts has been controversial. Many authors attributed the increase in the HDS and HDN activities to the increased acidity induced by fluorine, assuming that acidic sites catalyze C–S and C–N bond breaking (4–6). However, our previous study showed that fluorine hardly influenced the HDN of 2-methylcyclohexylamine, in which the nitrogen atom is removed by two kinds of C–N bond breaking, while it increased the HDN of o-toluidine, in which the hydrogenation of the phenyl ring was the rate-determining step (7). Apparently, the improved acidity does not play a key role in improving the HDN activity.

The influence of fluorine on the dispersion and sulfidation of active phases has been considered to explain the changes in the catalytic activity in HDS, HDN, and hydrogenation (6, 8–10). In some cases, the activities for thiophene HDS and alkene hydrogenation correlated very well with the change in the dispersion of the active phases (8, 9, 11), but in other cases there was no such correlation (11). Several X-ray photoelectron spectroscopy (XPS) studies found a slight decrease in the degree of sulfidation of molybdenum and tungsten upon addition of fluorine (8–10). By combining temperature-programmed sulfidation, XPS, and quick extended X-ray absorption fine structure techniques, we found that fluorine only slightly improved the overall sulfidation degree while it substantially aided the formation of a well-defined WS$_2$ structure during sulfidation (12, 13). We attributed the promotional effect of fluorine on the HDN of o-toluidine to the modification of the morphology of the active phases (14, 15).

High-resolution transmission electron microscopy (HRTEM) is a powerful technique for studying the changes in the morphology of active phases and has been applied in many studies of sulfide catalysts (6, 16–18). This Research Note presents the HRTEM results of our series of catalysts that were used in previous studies (12–15) to supplement our understanding of the role of fluorine in hydrotreating catalysts.

EXPERIMENTAL

Details of catalyst preparation were described in previous papers (12, 13). WO$_3$/Al$_2$O$_3$, WO$_3$/Al$_2$O$_3$–F, Ni–WO$_3$/Al$_2$O$_3$, and Ni–WO$_3$/Al$_2$O$_3$–F catalysts were made from ammonium metatungstate and calcined at 500°C, while ATT/Al$_2$O$_3$, ATT/Al$_2$O$_3$–F, Ni–ATT/Al$_2$O$_3$, and Ni–ATT/Al$_2$O$_3$–F catalysts were made from ammonium tetrathiotungstate (ATT) and were not calcined. The loading of tungsten was 10 wt% W in all catalysts, the loading of nickel
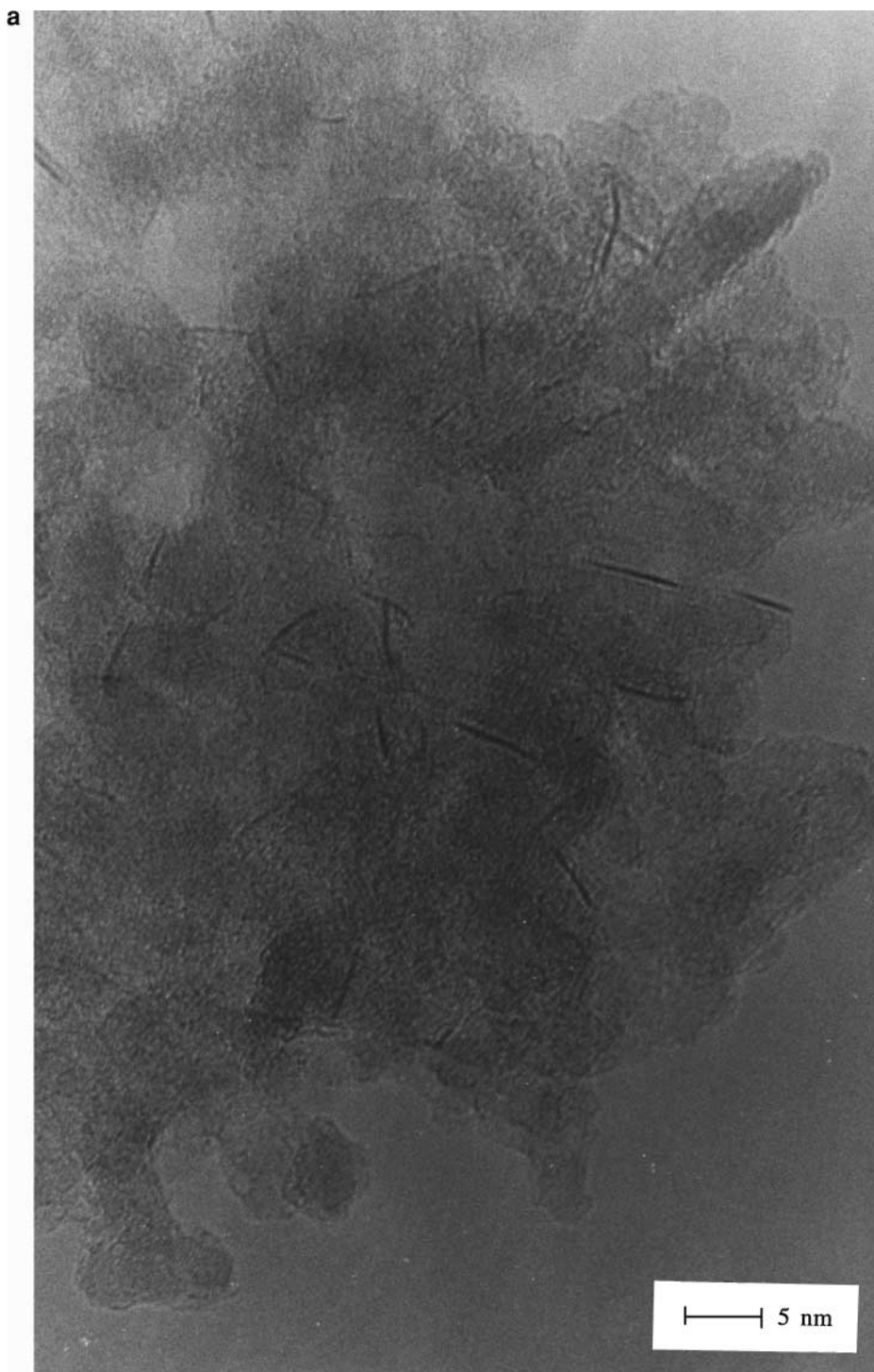
FIG. 1.   HREM micrographs of (a) WO$_3$/Al$_2$O$_3$ and (b) WO$_3$/Al$_2$O$_3$–F catalysts sulfided at 400°C for 4 h.

was 1 wt% Ni in nickel-promoted catalysts, and the load-ing of fluorine was 1 wt% F in fluorinated catalysts. Be-fore the HRTEM measurements, all catalysts were sulfided in a quartz reactor at 400°C for 4 h as described previ-ously (13). Then the sulfided samples were sealed in ni-

trogen (99.999%) until the HRTEM measurements were performed.

HRTEM measurements were carried out using a Philips CM30T transmission electron microscope with an LaB$_6$ fil-ament as electron source and operating at 300 kV. Samples
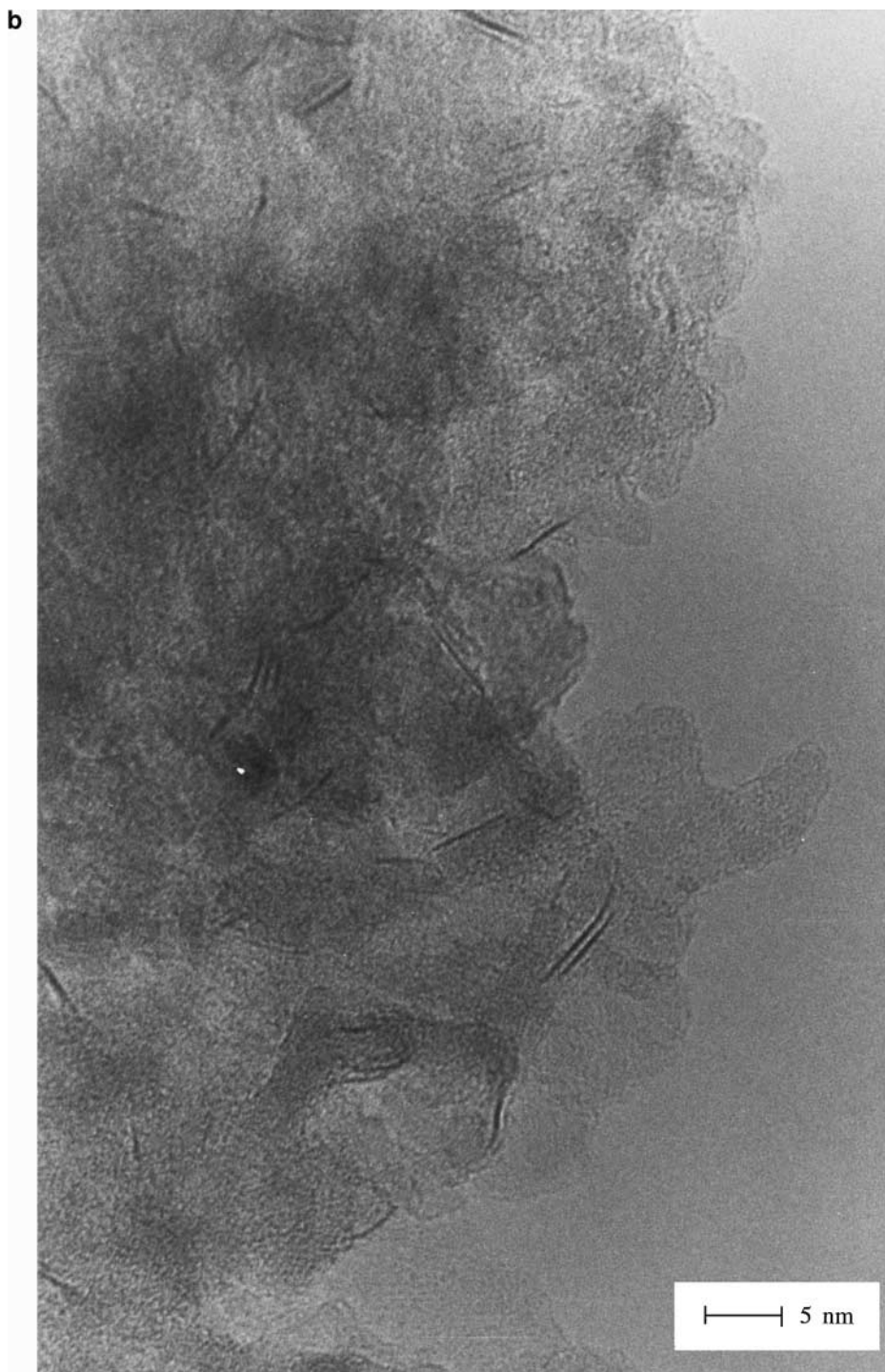
FIG. 1—*Continued*

were mounted on a microgrid carbon polymer supported on a copper grid by placing a few droplets of a suspension of the ground samples in *n*-hexane onto the grid, followed by drying at ambient conditions in an argon glovebox. Samples were transferred to the microscope in a special vacuum-transfer sample holder under exclusion of air (19).

RESULTS AND DISCUSSION

Figure 1 shows representative HRTEM micrographs of the (a) WO_3/Al_2O_3 and (b) WO_3/Al_2O_3–F catalysts. The black thread-like fringes correspond to the WS_2 slabs as has been shown in previous HRTEM studies (6, 16–18). On the micrograph of the fluorine-free catalyst sulfided at 400°C

for 4 h and published by Benitez *et al.* (6), only a few dark fringes were observed, which were hardly distinguishable, most of which were quite blurred or not well differentiated. Upon the incorporation of 1.5% fluorine into their catalyst, more WS_2 slabs were visible and multilayered crystallites as well as some exceptionally large aggregates of WS_2 were observed (Fig. 6 in Ref. 6). Our catalysts were prepared and sulfided under similar conditions, except that the tungsten loading was lower (10% vs 16.5% of tungsten) and the catalysts were not exposed to air before the TEM measurements. In our samples, the dark fringes, corresponding to WS_2 crystallites, are homogeneously dispersed on the support and no exceptionally large aggregates of WS_2 were observed. This enables a better evaluation of the effect of fluorine. The WS_2 slabs on the sulfided WO_3/Al_2O_3 catalyst (Fig. 1a) generally contain one layer, only a few have two layers. Most of the slabs in the WO_3/Al_2O_3–F catalyst (Fig. 1b) contain one layer, but more slabs with two and even three layers are observed than in the WO_3/Al_2O_3 catalyst.

In the sulfided $Ni–WO_3/Al_2O_3$ catalyst, most of the slabs are single-layered and well dispersed on the alumina support, as in the sulfided WO_3/Al_2O_3 catalyst. The same trend was observed for the effect of fluorine on the stacking of WS_2 (micrographs not shown): the fluorine-containing catalyst contained more multilayered slabs than the fluorine-free catalyst. Ramirez *et al.* found that, in their sulfided NiW/Al_2O_3 catalysts, most of the slabs had two layers, and that fluorine did not clearly increase the stacking of WS_2 (18). In their catalysts, nickel and tungsten were introduced simultaneously in a solution of nickel nitrate and ammonium metatungstate, the loadings of tungsten (16.5% W) and nickel (2.5% Ni) were much higher than in our catalysts (10% W and 1% Ni), and their catalysts were exposed to air before the TEM measurements. Our samples reveal more clearly the promotional effect of fluorine on the stacking of WS_2.

To make a quantitative comparison, statistical analyses were made based on several micrographs taken from different parts of the same sample, including 300 to 500 slabs. Figure 2 shows the statistical results of the distribution of the slabs with different stacking (Fig. 2a) and diameter (Fig. 2b). From these bar graphs it is clear that fluorine decreases the fraction of single-layered WS_2 slabs and increases the fraction of multilayered slabs. The average number of layers and the average diameter of WS_2 are listed in Table 1. Although the differences between the samples in slab diameter and stacking number are small, they are significant because a sufficient number of slabs was measured. Fluorine increases the average number of layers from 1.1 to 1.3 in the unpromoted catalysts and from 1.3 to 1.5 in the nickel-promoted catalysts. Most of the WS_2 slabs have a diameter between 20 and 40 Å. Fluorine shifts the distribution of WS_2 to a larger diameter; it increases the average diameter from 32 to 35 Å in unpromoted catalysts and from
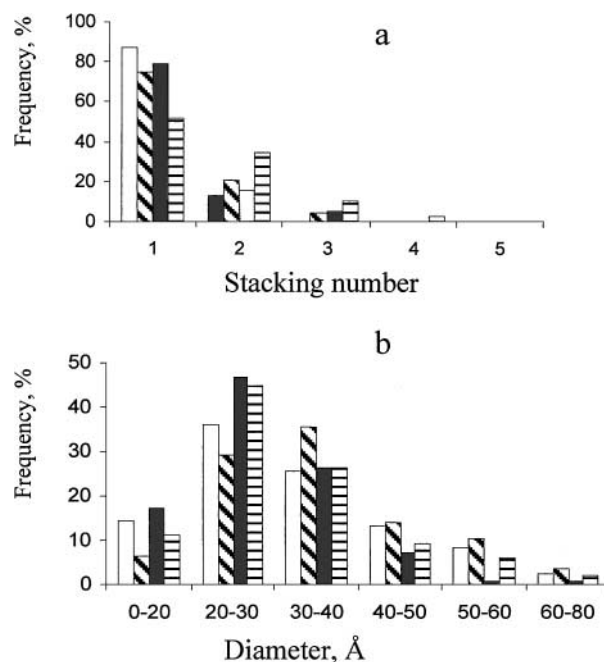

FIG. 2. (a) Stacking numbers and (b) diameters of WS_2 slabs in the (□) WO_3/Al_2O_3, (◨) WO_3/Al_2O_3–F, (■) $Ni–WO_3/Al_2O_3$, and (▤) and $Ni–WO_3/Al_2O_3$–F catalysts.

27 to 31 Å in nickel-promoted catalysts. Fluorine favors the formation of larger particles of WS_2, which is consistent with our previous results from other characterizations (12, 13, 20). A high content of fluorine reduces the surface area of the supported catalyst (8, 9). The 1% fluorine present in the catalysts used in this study did not cause a significant change in the surface area, however, and surface areas were 216, 212, 209, and 204 $m^2 g^{-1}$ for WO_3/Al_2O_3, WO_3/Al_2O_3–F, $Ni–WO_3/Al_2O_3$, $Ni–WO_3/Al_2O_3$–F, respectively (7).

Impregnation of alumina with an ammonium fluoride solution and subsequent calcination leads to the formation of aluminum-fluoride species on the support surface. The modification of the alumina influences the interaction between the catalyst precursor phase and the support and thus

TABLE 1

Average Number of Layers N and Diameter D of Various Catalysts

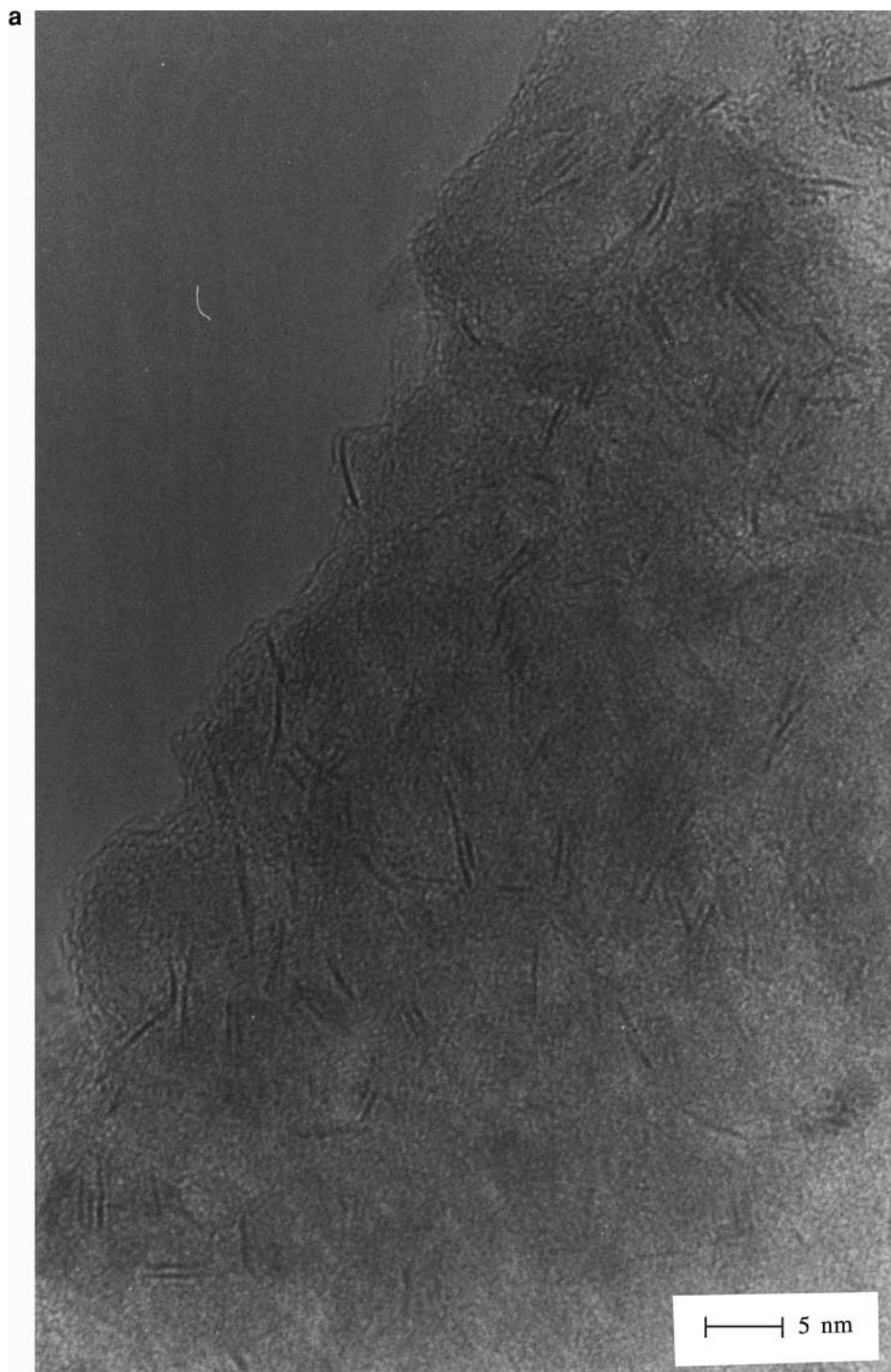| Catalysts	N	D, Å
WO_3/Al_2O_3	1.1	32
WO_3/Al_2O_3–F	1.3	35
$Ni–WO_3/Al_2O_3$	1.3	27
$Ni–WO_3/Al_2O_3$–F	1.5	31
ATT/Al_2O_3	1.5	33
ATT/Al_2O_3–F	1.7	31
$Ni–ATT/Al_2O_3$	1.7	32
$Ni–ATT/Al_2O_3$–F	2.0	33

FIG. 3. HREM micrographs of (a) ATT/Al$_2$O$_3$ and (b) ATT/Al$_2$O$_3$–F catalysts sulfided at 400°C for 4 h.

the sulfidation of the supported catalyst (12, 13). FT–IR studies have shown that fluorine substitutes for hydroxyl groups on the alumina surface (21). Different types of hydroxyl groups are present on the alumina surface (22, 23) which have different tendencies to be replaced by fluorine and form different types of aluminum-fluoride species. An

NMR study detected three types of Al–F species on fluorinated alumina (24). Further work is required, however, to understand the structures of these Al–F species and how they affect the sulfidation of the supported catalyst.

On the micrographs of the (Fig. 3a) ATT/Al$_2$O$_3$ and (Fig. 3b) ATT/Al$_2$O$_3$–F catalysts one can see many more
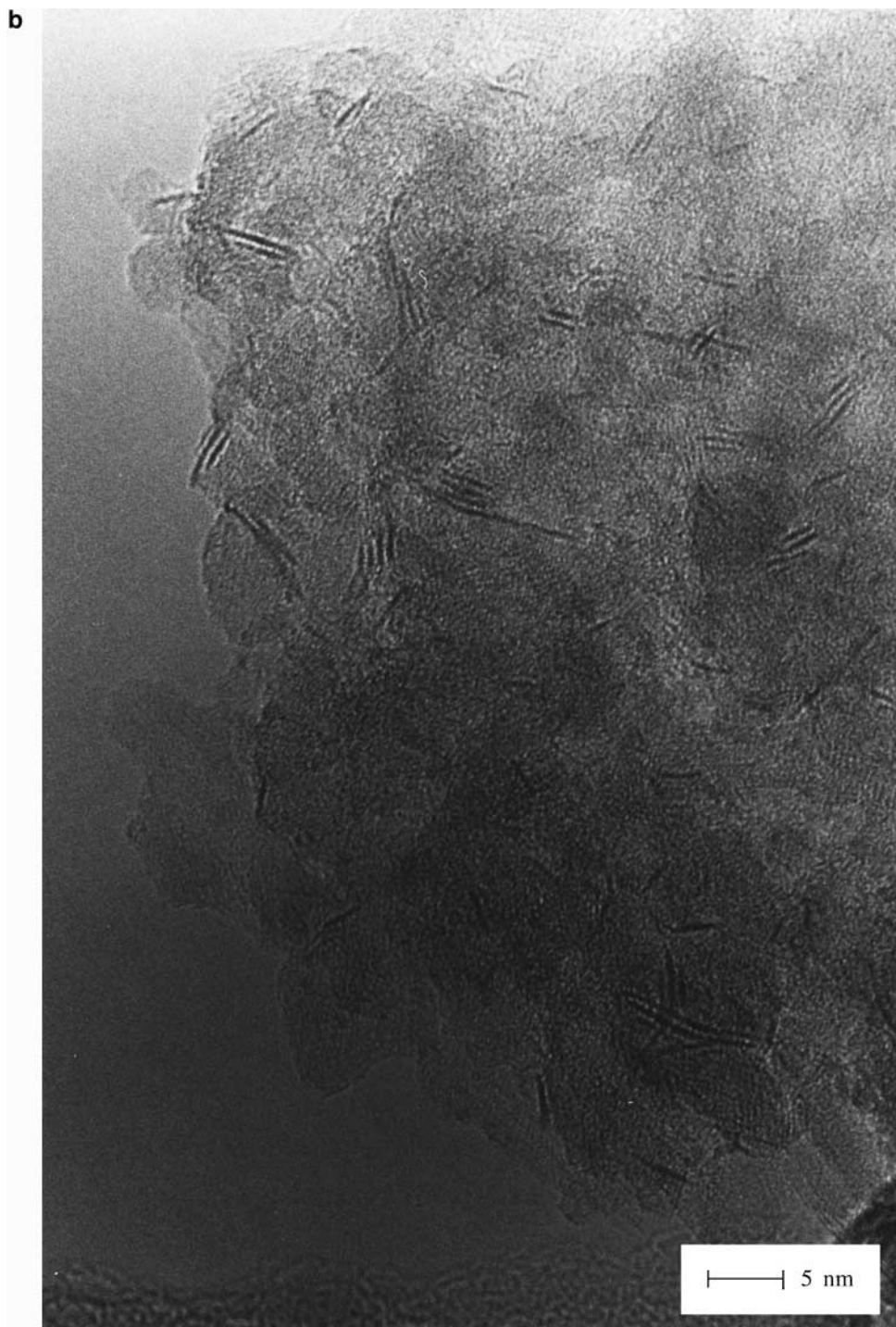
b

FIG. 3—*Continued*

multilayered WS$_2$ slabs than on the WO$_3$ catalysts (Fig. 1). Previous characterization results showed that the catalysts prepared from ATT were fully sulfided while the catalysts prepared from ammonium metatungstate were only partially sulfided under the same sulfidation conditions (12, 13). The results of the statistical analysis (Fig. 4) confirm that the fraction of single-layered slabs is much smaller on ATT catalysts than on the WO$_3$ catalysts. The average number of WS$_2$ stacking layers in all the ATT catalysts is much larger than that of the corresponding WO$_3$ catalysts (Table 1). This means that one can produce more highly stacked WS$_2$ catalysts by using ammonium tetrathiotungstate and omitting
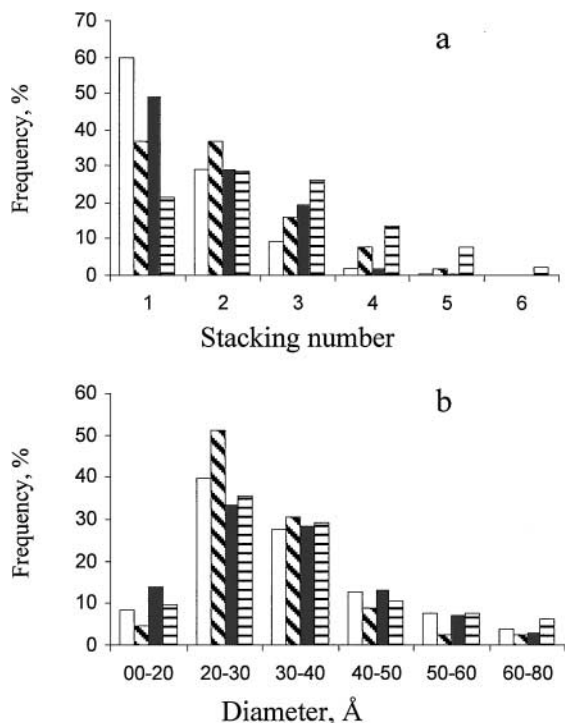
FIG. 4. (a) Stacking numbers and (b) diameters of WS_2 slabs in the (□) ATT/Al_2O_3, (◥) ATT/Al_2O_3–F, (■) Ni–ATT/Al_2O_3, (⊟) and Ni–ATT/Al_2O_3–F catalysts.

calcination. Addition of fluorine to the ATT/Al_2O_3 catalyst can still increase the fraction of multi-layered WS_2. Fluorine does not change the average diameter of the WS_2 crystallites to a great extent, but it slightly decreases the fraction of WS_2 slabs shorter than 20 Å due to its promotional effect on the formation of a well-defined WS_2 structure (12, 13).

In the Ni–ATT catalyst, fluorine shows effects similar to the unpromoted ATT catalyst (Fig. 4 and Table 1). In an HRTEM study of NiW/Al_2O_3 catalysts prepared from ammonium tetrathiotungstate and nickel nitrate via one-step impregnation, abnormally large WS_2 structures were observed (18), which was not the case in our study. Their samples were only treated at 127°C in a flow of H_2S/H_2 (18). We observed that ammonium tetrathiotungstate on alumina does not decompose completely in H_2S/H_2 to WS_2 below 300°C (12, 13). This explains why a large excess of sulfur and $(NH_4)_2WS_4$ crystals were still observed in the samples described by Ramirez *et al.* (18).

Comparing the nickel-promoted catalysts with their unpromoted counterparts (Figs. 2 and 4), one observes that nickel increases the stacking number just as fluorine does. Its influence on the diameter is opposite to that of fluorine; however, nickel increases the fraction of WS_2 crystallites shorter than 20 Å. The effect of nickel on the diameter of WS_2 can be explained by the process of sulfidation of

NiW/Al_2O_3 catalysts (13, 25, 26). Sulfidation of nickel starts at room temperature, while the formation of WS_2 does not occur to a significant extent below 300°C (13, 26). Upon the formation of WS_2, nickel sulfide tends to combine with WS_2. The decoration of nickel at the edges of WS_2 slabs prevents the further growth of WS_2 crystallites during sulfidation at higher temperature.

In the investigation of the promotional effect of fluorine on HDN reactions, it was found that fluorine preferentially improved the hydrogenation of the aromatic ring, while the hydrogenation of the alkene and $C(sp^3)$–N bond breaking were hardly affected (7). Our kinetic studies indicated that fluorine did not change the intrinsic properties of the active sites for the HDN of MCHA and o-toluidine (14, 15). This has been explained by assuming that the saturation of the aromatic ring is a stacking-sensitive reaction, and that higher stacking favors the adsorption of the aromatic ring on the active site via its π-electron (7, 15). The promotional effect of fluorine on the HDN of o-toluidine is mainly due to the increase in the number of stacking layers of WS_2. The present results confirm our explanation of the kinetic data.

CONCLUSION

The influence of fluorine on the morphology of WS_2 on an alumina support was investigated by means of HRTEM. Fluorine favors the formation of WS_2 slabs with higher stacking and reduces the number of WS_2 slabs smaller than 20 Å. Using ammonium tetrathiotungstate instead of ammonium metatungstate results in many more multilayered WS_2 slabs and suppresses the formation of WS_2 crystallites smaller than 20 Å. Incorporation of nickel into the tungsten-only catalysts increases the fraction of WS_2 slabs with higher stacking, and, at the same time, it increases the number of small crystallites smaller than 20 Å. Higher stacking of WS_2 favors the hydrogenation of the phenyl ring in the hydrodenitrogenation of o-toluidine, which is the rate-determining step.

REFERENCES

1. Holm, V. C. F., and Clark, A., *Ind. Eng. Chem. Prod. Res. Dev.* **2**, 38 (1963).
2. Gerberich, H. R., Lutinski, F. E., and Hall, W. K., *J. Catal.* **6**, 209 (1966).
3. Covini, R., Fattore, V., and Giordano, N. J., *J. Catal.* **7**, 126 (1967).
4. Boorman, P. M., Kriz, J. F., Brown, J. R., and Ternan, M., *in* "Proc. 4th Int. Climax Conf. on Chemistry and Uses of Molybdenum" (H. F. Barry and P. C. H. Mitchell, Eds.), p. 192, Ann Arbor, 1982.
5. Jiratova, K., and Kraus, M., *Appl. Catal.* **27**, 21 (1986).
6. Benitez, A., Ramirez, J., Vazquez, A., Acosta, D., and Lopez Agudo, A., *Appl. Catal. A* **133**, 103 (1995).
7. Sun, M., Bussell, M. E., and Prins, R., *Appl. Catal. A* **216**, 103 (2001).
8. Papadopoulou, Ch., Lycourghiotis, A., Grange, P., and Delmon, B., *Appl. Catal.* **38**, 255 (1988).
9. Matralis, H. K., Lycourghiotis, A., Grange, P., and Delmon, B., *Appl. Catal.* **38**, 273 (1988).

10. Benitez, A., Ramirez, J., Fierro, J. L. G., and Lopez Agudo, A., *Appl. Catal. A* **144**, 343 (1996).

11. Ramirez, J., Cuevas, R., Lopez Agudo, A., Mendioroz, S., and Fierro, J. L. G., *Appl. Catal.* **57**, 223 (1990).

12. Sun, M., Bürgi, Th., Cattaneo, R., and Prins, R., *J. Catal.* **197**, 172 (2001).

13. Sun, M., Bürgi, Th., Cattaneo, R., van Langeveld, A. D., and Prins, R., *J. Catal.* **201**, 258 (2001).

14. Sun, M., and Prins, R., *J. Catal.* **201**, 138 (2001).

15. Sun, M., and Prins, R., *J. Catal.* **203** (2001), doi:10.1006/jcat.2001.3297.

16. Sanders, J. V., *in* "Catalysis, Science and Technology" (J. R. Anderson and M. Boudart, Eds.), Vol. 7, p. 51. Springer-Verlag, Berlin, 1985.

17. Payen, E., Hubaut, R., Kasztelan, S., Poulet, O., and Grimblot, J., *J. Catal.* **147**, 123 (1994).

18. Ramirez, J., Castillo, P., Benitez, A., Vazquez, A., Acosta, D., and Lopez Agudo, A., *J. Catal.* **158**, 181 (1996).

19. Zandbergen, H. W., Kooyman, P. J., and van Langeveld, A. D., *in* "Proceedings 14th Int. Conference on Electron Microscopy," 1998, Cancun, Mexico, Vol. II, p. 491.

20. Schwartz, V., Sun, M., and Prins, R., *J. Phys. Chem. B*, in press.

21. Okamoto, Y., and Imanaka, T., *J. Phys. Chem.* **92**, 7102 (1988).

22. Knözinger, H., and Ratnasamy, P., *Catal. Rev. Sci. Eng.* **17**, 31 (1978).

23. Tsyganenko, A. A., and Mardilovich, P. P., *J. Chem. Soc. Faraday Trans.* **92**, 4843 (1996).

24. Fischer, L., Harle, V., Kasztelan, S., and d'Espinose de la Caillerie, J. B., *Solid State Nucl. Magn. Reson.* **16**, 85 (2000).

25. Reinhoudt, H. R., van Langeveld, A. D., Kooyman, P. J., Stockmann, R. M., Prins. R., Zandbergen, H. W., and Moulijn, J. A., *J. Catal.* **179**, 443 (1998).

26. Kishan, G., Coulier, L., de Beer, V. H. J., van Veen, J. A. R., and Niemantsverdriet, J. W., *J. Catal.* **196**, 180 (2000).